Percolative $c(2\times2)$ adlayer structure in nonequilibrium adsorption models

J. W. Evans and D. E. Sanders
Ames Laboratory, Iowa State University, Ames, Iowa 50011
(Received 15 June 1988)

We consider simple adsorption models describing two systems [H_2O on Fe(001) and O_2 on Pd(100)] in which $c(2\times2)$ short-range order is formed *during* chemisorption, and metastable saturation states result. This ordering is characterized using concepts from correlated percolation theory. Rapid increases in average domain size near saturation are associated with "ghost percolation thresholds" just above saturation. Generalizing these adsorption models to include an island-forming propensity, α, is shown to move the saturation state closer to $c(2\times2)$ percolation. The $\alpha\rightarrow\infty$ behavior is elucidated by analyzing corresponding "continuum two-phase grain growth models" using ideas from stochastic geometry, continuum, and random lattice percolation theory.

I. INTRODUCTION

Equilibrium ordering in commensurately chemisorbed adlayers[1] and, more recently, the evolution of order during equilibration at constant coverage (e.g., following a rapid quench),[2] have been elucidated using various powerful statistical-mechanical concepts and techniques. However, there has been little study of the evolution of order *during* chemisorption, or of metastable states resulting from the kinetic limitations of low surface mobility.[3–6] Here we consider various simple irreversible filling models describing the development of $c(2\times2)$ short-range order during chemisorption. These will be described in detail below. The strongly model-dependent local structure and structure on the characteristic or correlation length scale, together with the associated diffracted intensity behavior, have been analyzed previously.[5,6] Here we focus on the more universal structure and behavior associated with longer length scales. Specifically, we characterize the dependence of various nonlocal measures of domain size on coverage (Θ monolayers). We also characterize the ramified, fractal large-scale domain structure, which is most dramatic in the metastable saturation states. These studies are facilitated via adaption and extension of ideas from percolation theory.

We first introduce the concepts necessary for a quantitative characterization of disordered $c(2\times2)$ structure. In perfect $c(2\times2)$ ordering on a square lattice, adspecies occupy one of two $(\sqrt{2}\times\sqrt{2})R45°$ sublattices (Fig. 1), and are correspondingly assigned one of two "phases," $\pm$, say. For the disordered $c(2\times2)$ distributions considered here, no nearest-neighbor (NN) pairs of sites are filled, and the fractional coverage $\Theta^{\pm}$ for adspecies of both "phases" are equal (on an infinite lattice). We emphasize that the phase here only refers to the sublattice on which an adspecies resides. It does *not* mean "thermodynamic phase." [For example, clearly the ordered $c(2\times2)$ thermodynamic phase of the hard-square lattice gas includes adspecies on both sublattices.]

Various "connectivity rules" could be involved to describe $c(2\times2)$ domains.[6] We could say that adspecies belong to the same domain if they are connected by second, i.e., diagonal NN bonds (2NN connectivity). Alternatively, second or third NN bonds could suffice to connect adspecies in the same domain. The latter corresponds to longer-range so-called *AB* connectivity, where *A* (*B*) denotes empty (filled) sites, and domains are associated with connected clusters of NN *AB* bonds.[7] Clearly 2NN domains can link to form larger *AB* domains (Fig. 1). For either connectivity choice, domains of different phase cannot cross, so $c(2\times2)$ *domain percolation* on an infinite lattice *is impossible* for reasons of topology and symmetry.[6] We note here that more complicated connectivity rules are generally required to relate domain structure to other, e.g., thermodynamic, properties of the adlayer.[8,9]

Next we discuss various quantitative measures of domain size.[10] Let n_s denote the number, and R_s the average radius of gyration, of domains with exactly s adspecies (given a choice of connectivity rule). Then define the average domain size (number of adspecies), s_{av}, by

$$s_{av}=\sum_s s^2 n_s \Big/ \sum_s s n_s \ , \tag{1}$$

and average radii of gyration, $R_{av}(i)$, for $i=1$ and 2, by

$$R^2_{av}(i)=\sum_s R_s^2 s^i n_s \Big/ \sum_s s^i n_s \ . \tag{2}$$

The connectivity length, measuring the average separation between two adspecies in the same domain, is given by $\sqrt{2}R_{av}(2)$.[10] We also consider the effective dimen-

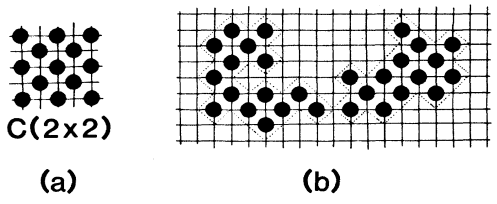

FIG. 1. (a) Perfect $c(2\times2)$ ordering. (b) Two 2NN domains linking to form a single *AB* domain.

sion, $\bar{d}$, for domains, which typically differs from the lattice dimension of 2. We determine $\bar{d} \equiv \rho^{-1}$ from the slope, ρ, of a $\ln R_s$ versus $\ln s$ plot for large s ($\gtrsim 50$), rather than the strict $s \to \infty$ value of the slope.[10] In previous diffraction studies we have invoked "chord length measures" of domain size, e.g., the average number of adspecies in horizontal (or vertical) double-spaced strings, or in diagonal strings.[5]

Domain perimeter structure is also of interest. Let t_s denote the average number of empty perimeter sites second NN to filled sites in domains of s adspecies. In the models considered here, for fixed Θ, t_s/s decreases smoothly as $s \to \infty$ to a nonzero limit, R, which measures domain ramification.[10]

There have been many studies of the divergent behavior of s_{av} and $R_{av}(i)$ for model systems incorporating percolation transitions.[10] Various connectivity rules have been considered.[11] Most studies have assumed a random distribution of occupied sites (or bonds). More recently, equilibrium (Ising and Potts model) and various nonequilibrium prescriptions of correlations have also been considered.[7-9,12-16] However, this study differs fundamentally in that the physical models do *not* incorporate a percolation transition. Instead we shall characterize the behavior of these filling models in terms of a "ghost percolation transition" occurring slightly above the saturation coverage. To further elucidate this structure, we also adopt another approach suggested previously,[6,15] which involves imbedding the physical filling process into a larger class in which the ghost transition becomes real. Here this is achieved by biasing the filling of one phase over the other.

Various standard techniques can then be used to analyze such (real) transitions. Here we adopt powerful finite-size-scaling (FSS) procedures,[17] which we now describe briefly. Suppose a transition occurs at some critical value, δ_c, of some bias parameter δ. The δ dependence of the average $c(2\times2)$ domain size for an $L \times L$ lattice with periodic boundary conditions is assumed to satisfy[17]

$$M_L(\delta) \sim L^{2+\gamma/\nu} G((\delta-\delta_c)L^{1/\nu}) , \tag{3}$$

where $G(z) \sim z^{-\gamma}$ as $z \to \infty$, and γ (ν) is the scaling exponent for s_{av} (the connectivity length). Then intersection points of the ratio functions $R_L(\delta) = M_{2L}(\delta)/M_L(\delta)$ for different L should approach δ_c, as $L \to \infty$. Convergence will be slower for systems with longer-range correlations. Their values at these points should approach $2^{2+\gamma/\nu}$. All calculations here suggest random percolation values for scaling exponents, which is expected for finite-range correlations. Thus we shall only report estimates of δ_c determined from where $R_L(\delta)$ equals the random percolation value, $2^{273/72}$, of $2^{2+\gamma/\nu}$.[10]

In Sec. II we analyze the five-site model where empty sites on a square lattice fill randomly provided all four NN are empty. A related eight-site model is analyzed in Sec. III where 2NN pairs of sites fill randomly provided all six NN sites are empty. The effect of introducing an island-forming propensity into the five-site model is considered in Sec. IV. Finally, in Sec. V we summarize our findings, and discuss some extensions of these ideas.

II. FIVE-SITE FILLING MODEL: DISORDERED $c(2\times2)$O/Fe(001)

In this five-site model empty sites on a square lattice are irreversibly filled at random provided all four NN sites are empty. Filling continues up to a saturation coverage, Θ_s, of 0.364 (Refs. 18–20) where there remain no empty sites with all NN empty. References 5, 6, 18, and 20 examine the behavior of various local quantities and the diffracted intensity for this model, which was proposed to describe the formation of metastable $c(2\times2)$O/Fe(001) following exposure of Fe(001) to H_2O.[18]

Here we rely on computer simulation to study nonlocal domain structure for both 2NN and *AB* connectivity. We find surprisingly large domains in the saturation state with $s_{av} \sim 165$, $R_{av}(2) \sim 21$, and $R_{av}(1) \sim 13.3$ for 2NN connectivity (see Fig. 2). Many trials on large lattices are required to reduce uncertainly due to large statistical fluctuations especially at saturation (where we use 100 trials on a 300×300 lattice). Our uncertainties are $\pm 6\%$. The situation is much worse for *AB* connectivity, where domains are much larger, e.g., $s_{av} \gtrsim 1200$ at Θ_s where finite-size effects significantly influence our 400×400 lattice results.

A dramatic increase in s_{av} and $R_{av}(i)$ is observed near Θ_s due to extensive linkage of smaller domains. In fact, one might anticipate that analytic extension of these quantities to $\Theta \geq \Theta_s$ would produce a *divergence* at a coverage Θ_{GP}, somewhat above Θ_s, characterized by appropriate random percolation critical exponents. We describe Θ_{GP} as a "ghost percolation threshold" since this divergence is not realized in the physical coverage range. Thus we write (cf. Ref. 10)

$$\begin{aligned} s_{av} &= [(1-\Theta/\Theta_{GP})F_0(\Theta)]^{-\gamma} , \\ R_{av}(1)^2 &= A_1\Theta[(1-\Theta/\Theta_{GP})F_1(\Theta)]^{-2\nu+\beta} , \\ R_{av}(2)^2 &= A_2\Theta[(1-\Theta/\Theta_{GP})F_2(\Theta)]^{-2\nu} , \end{aligned} \tag{4}$$

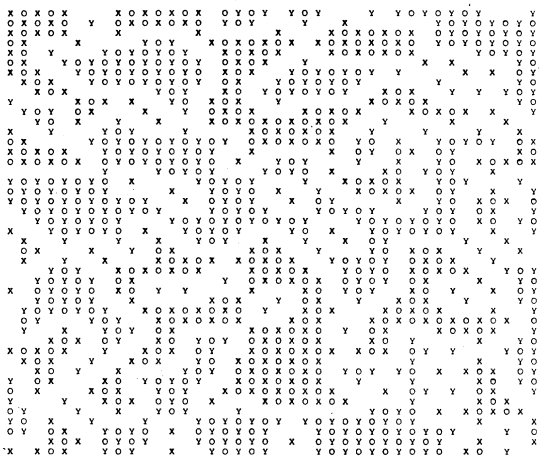

FIG. 2. Saturation state of the five-site model (random filling with NN blocking). *X* and *Y* denote filled states of different phase. Empty sites within domains are denoted by 0.

where $\gamma=\frac{43}{18}$, $\nu=\frac{4}{3}$, $\nu-\beta/2=\frac{91}{72}$. The $F_i\to1$, as $\Theta\to0$, and are nonzero at $\Theta=\Theta_{GP}$. We have also used results from formal Θ expansions[20] to incorporate exact low-Θ behavior, $R_{av}(i)^2\sim A_i\Theta$, where $A_1=2$ (6) and $A_2=4$ (12) for 2NN (AB) connectivity.

These ghost percolation ideas are supported by Fig. 3 where we have plotted simulation values of $s_{av}^{-1/\gamma}$, $[R_{av}(1)^2/(A_1\Theta)]^{-1/(2\nu-\beta)}$, $[R_{av}(2)^2/(A_2\Theta)]^{-1/(2\nu)}$ against Θ. A common zero, Θ_{GP}, of the extrapolated functions is certainly compatible with the data. Using a least-squares polynomial fit (weighting high Θ points more heavily), we estimate that $\Theta_{GP}=0.43$ (0.41) for 2NN (AB) connectivity. This procedure also yields polynomial approximations to the F_i which, in conjunction with (4), provide simple formulas for s_{av} and $R_{av}(i)$. These reproduce simulation data for s_{av} and $R_{av}(i)$ to within at worst $\pm6\%$ uniformly over $0\le\Theta\le\Theta_s$. For 2NN connectivity, we obtain $F_i=1+a_i\Theta+b_i\Theta^2$ with $a_i=1.17,1.06,0.97$ and $b_i=-4.97,-4.88,-4.65$ for $i=0,1,2$, respectively. For AB connectivity, we obtain $F_i=1+a_i\Theta+b_i\Theta^2+c_i\Theta^3$ with $a_i=-0.27,0.96,0.93$, $b_i=-7.55,-11.7,-12.5$, and $c_i=11.4,16.9,19.9$ for $i=0,1,2$, respectively.

Next we describe the Θ dependence of the ramification, $R=\lim_{s\to\infty} t_s/s$, and effective dimension, $\bar{d}$, of large domains. First we consider the low-Θ regime. One can readily verify that formal Θ expansions[21] for the various $c(2\times2)$ domain (cluster) probabilities exhibit lead coefficients *independent* of domain shape. Thus as $\Theta\to0$, domains exhibit random animal statistics even for this constrained filling problem. Thus the structure of these $c(2\times2)$ animals with 2NN (AB) connectivity corresponds to that of standard random animals with NN (NN+2NN) connectivity. For the former, values for $R=1.20$ and $\rho=0.64$ have been reported previously.[22] We find that R and ρ decrease with Θ to saturation values of $R=0.83$ (0.92) and $\rho\approx0.59$ (0.57), for 2NN (AB) connectivity. The most rapid decrease is near Θ_s

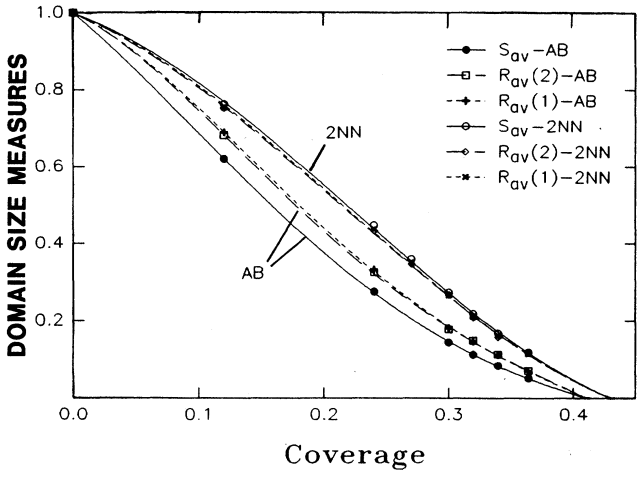

FIG. 3. Simulation results for the Θ dependence of $s_{av}^{-1/\gamma}$, $[R_{av}(1)^2/(A_1\Theta)]^{-1/(2\nu-\beta)}$, and $[R_{av}(2)^2/(A_2\Theta)]^{-1/(2\nu)}$ for the five-site model for both 2NN and AB connectivity.

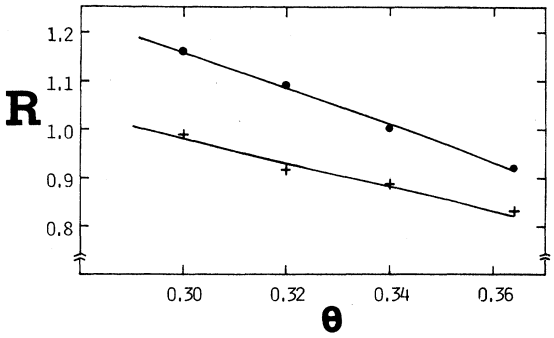

FIG. 4. Near-saturation Θ dependence of R for the five-site model with 2NN (+) and AB (●) connectivity.

analogous to random percolation behavior.[10] (See Fig. 4 for R values.) R values are larger for AB than 2NN connectivity indicating that strings of 2NN domains constituting the largest AB domains include some "smaller" 2NN domains. For completeness, Fig. 5 shows saturation values of perimeter length (t) to size (s) ratios for many 2NN domains.

One approach to elucidate the ghost percolative behavior involves imbedding the physical adsorption model into a larger class which incorporates a $c(2\times2)$ percolation transition.[6,15] In this class, the filling rates, $k^{\pm}=(1\pm\delta)k$, for the two $\pm$ $c(2\times2)$ phases differ for nonzero "bias" δ. Consider first percolation for a *2NN connectivity* choice. A finite-size-scaling (FSS) analysis of saturation states reveals a percolation transition at critical bias $\delta_c=0.160\pm0.002$ (with $\Theta^+/\Theta=0.636$). Random percolation critical exponents are found (as is the case for all our analyses). As δ increases from 0 to δ_c for these saturation states, R drops further to 0.72, and ρ appears to approach the random percolation threshold value of 0.53 (as determined by the critical exponents[10]) Next consider the case $\delta=1$ which corresponds to random filling on the square + phase sublattice with $\Theta_s=\frac{1}{2}$. Clearly, here 2NN percolation occurs at $\Theta=\Theta'/2$ where $\Theta'=0.5927$ is the standard random site percolation

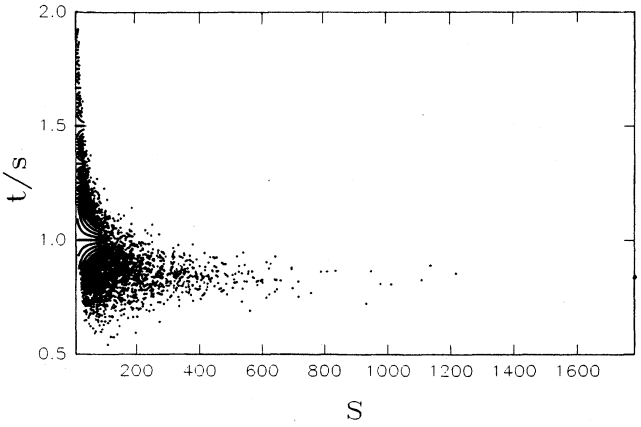

FIG. 5. Perimeter length (t) to size (s) ratios for 2NN domains in the five-site model at saturation.

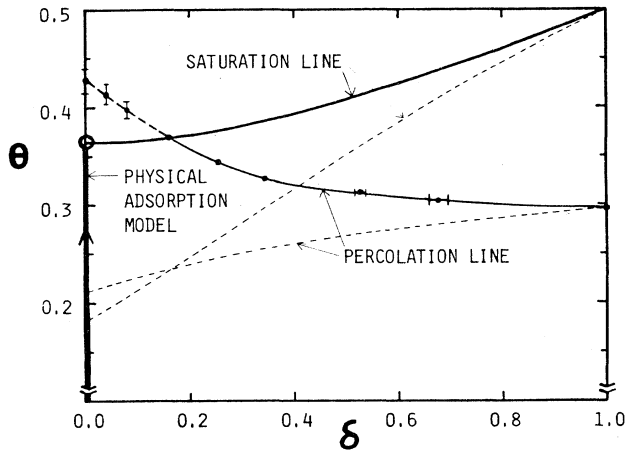

FIG. 6. Percolation phase diagram for the five-site model with bias, δ. Dashed lines show values of the majority phase partial coverage corresponding to percolation and saturation.

threshold for a square lattice.[10]

The percolation phase diagram, Fig. 6, provides a complete picture of percolation in these models. The percolation line running from $(\delta,\Theta)=(1,0.296)$ to the saturation state $(\delta,\Theta)=(0.160,0.367)$ is accurately determined by FSS analysis at fixed Θ (see Table I). The zeros of $s_{av}^{-1/\gamma}$ extrapolated to $\Theta \geq \Theta_s$, for various fixed $\delta < \delta_c$ (as described for $\delta=0$ above), determine the natural extension of the percolation line back to $\delta=0$. The proximity of this "ghost percolation line" to the physical ($\delta=0$) saturation state explains the percolative features of the latter.

In an analogous treatment for *AB connectivity,* one finds a much smaller critical bias for the saturation state of $\delta_c=0.065\pm0.001$ (Ref. 23) (with $\Theta^+/\Theta=0.555$). For $\delta=1$, percolation now occurs at $\Theta=\Theta''/2$, where $\Theta''=0.407$ is the random site percolation threshold for NN+2NN connectivity on a square lattice.[11] Thus in the percolation phase diagram, the percolation line now runs between $(\delta,\Theta)=(1,0.204)$ and the saturation state $(\delta,\Theta)=(0.065,0.365)$, and extends back to $(\delta,\Theta)=(0,0.41)$. It is closer to the physical saturation state than for 2NN connectivity.

TABLE I. Determination of critical bias for $c(2\times2)$ 2NN percolation in the five-site model at saturation, and for fixed Θ; δ values satisfying $R_L(\delta)=2^{273/72}$ are shown.

Θ	$L=16$	$L=32$	$L=64$
saturation	0.160	0.158	0.160
$\frac{44}{128}$	0.233	0.244	0.251
$\frac{42}{128}$	0.324	0.343	0.346
$\frac{40}{128}$	0.487	0.515	0.528
$\frac{39}{128}$	0.649	0.674	0.675

III. EIGHT-SITE FILLING MODEL: METASTABLE $c(2\times2)$O/Pd(100)

The percolative features described above for the five-site model should be shared by other microscopic adsorption models which produce disordered $c(2\times2)$ distributions. To support this claim, here we consider the eight-site model proposed to describe the formation of metastable $c(2\times2)$O/Pd(100) at low Pd temperature and high O_2 pressure:[6,24] dissociative adsorption of O_2 occurs at 2nd NN pairs of empty sites provided all six NN sites are empty; we assume adatoms are immobile (but more general models have been considered[6]). Here we augment previous studies with more extensive simulation results and FSS analyses which parallel those of Sec. II. Results are presented only for the 2NN connectivity choice.

The dramatic increase in domain size near saturation, $\Theta_s=0.362$, where $s_{av}\sim280$, $R_{av}(2)\sim29$, $R_{av}(1)\sim19$,[6] is again associated with a ghost percolation threshold, Θ_{GP}, somewhat above Θ_s. Incorporating the correct low-Θ behavior, we write

$$s_{av}=2[(1-\Theta/\Theta_{GP})F_0(\Theta)]^{-\gamma},$$
$$R_{av}(1)^2=\tfrac{1}{2}[(1-\Theta/\Theta_{GP})F_1(\Theta)]^{-2\nu+\beta}, \quad (5)$$
$$R_{av}(2)^2=\tfrac{1}{2}[(1-\Theta/\Theta_{GP})F_2(\Theta)]^{-2\nu},$$

where the critical exponents assume random percolation values, and the $F_i\to0$, as $\Theta\to1$, and are nonzero at Θ_{GP}. Simulation data for s_{av} and $R_{av}(i)$ is compatible with a common Θ_{GP} of about 0.43 for these quantities (see Fig. 7). This data is reproduced to within at worst ±7% uniformly over $0\leq\Theta\leq\Theta_s$ using the following polynomial fits to $F_i=1+a_i\Theta+b_i\Theta^2$: $a_i=1.26,-0.81,-2.37$ and $b_i=-5.06,-1.62,2.02$, for $i=0,1,2$, respectively.

Saturation values of $R=0.72$ and $\rho=0.60$ have been reported previously.[6] Figure 8 shows saturation values of perimeter length (t) to size (s) ratio for many 2NN domains. Note that R and ρ decrease with Θ, most

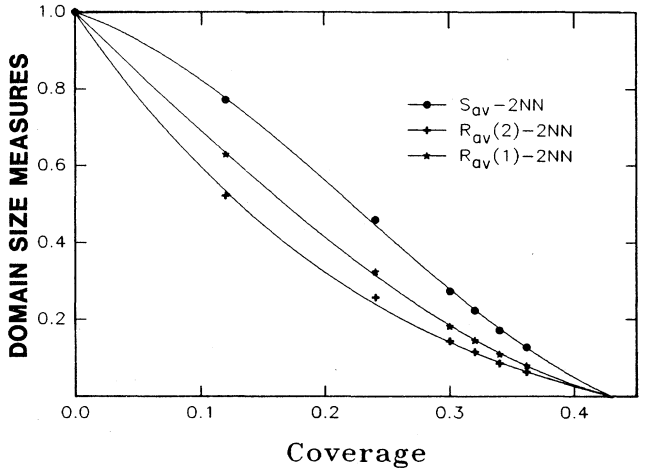

FIG. 7. Simulation results for the Θ dependence of $(s_{av}/2)^{-1/\gamma}$, $[2R_{av}(1)^2]^{-1/(2\nu-\beta)}$, and $[2R_{av}(2)^2]^{-1/(2\nu)}$ for 2NN domains in the eight-site model.

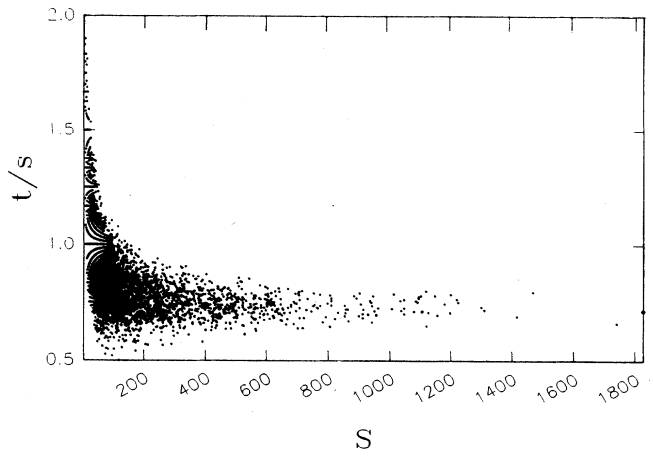

FIG. 8. Perimeter length (t) to size (s) ratios for 2NN domains in the eight-site model at saturation.

quickly near Θ_s, just as in the five-site model. However, in this eight-site model, the structure of domains as $\Theta\to 0$ is described by correlated square lattice animals built randomly from dimers (occupying NN pairs of sites), rather than from monomers.[6,16]

A complete percolation phase diagram can be constructed analogous to Sec. II. Note that adatoms from each diatom fill sites of only one $c(2\times2)$ phase. We bias the adsorption rates, $k^{\pm}=(1\pm\delta)k$, for different $\pm$ phases, as previously.[6] FSS analysis shows that a $c(2\times2)$ percolation transition occurs in the saturation states for critical bias $\delta_c=0.16$ (Ref. 25) (with $\Theta^{+}/\Theta=0.63$). Note that $\delta=1$ corresponds to dimer adsorption onto NN sites of the square + phase sublattice. Here saturation occurs at $\Theta_s=\Theta^{*}/2$, and percolation $\Theta=\Theta'''/2$, where $\Theta^{*}=0.9068$ and $\Theta'''=0.562$ denote the jamming coverage and filled site percolation threshold, respectively, for random dimer filling of NN pairs of sites on a square lattice. The former is an old result,[26] but the latter is new.[27] Thus in the percolation phase diagram, the percolation line runs between $(\delta,\Theta)=(1,0.281)$ and the saturation state $(\delta,\Theta)=(0.16,0.365)$, and extends back to $(\delta,\Theta)=(0,0.43)$. Only the saturation line differs qualitatively from the five-site model.

IV. INFLUENCE OF $c(2\times2)$ ISLAND-FORMING PROPENSITY ON DOMAIN PERCOLATIVE STRUCTURE

Models for the two adsorption processes described above involve only *random* adsorption, subject to certain blocking constraints (which could be associated with infinitely repulsive NN adspecies interactions). Clearly this is a first approximation. Consider chemisorption via a physisorbed precursor. In general, the density of this precursor, and thus the adsorption rates, will be influenced by interactions between precursor species and nearby chemisorbed species.[4] In particular, attractive interactions will enhance chemisorption near island edges, thus producing an island-forming propensity (see the simulations in Ref. 4). For example, in systems with strongly repulsive NN interactions, attractive 2NN interactions could lead to a $c(2\times2)$ island-forming propensity. Since many systems fit into this category, we are motivated to study below some corresponding simple adsorption models. Finally we note that the total adsorption rate for island-forming processes will increase (induction) after nucleation and growth of the "first few" islands. In contrast, the total adsorption rates for the processes discussed in Secs. II and III decrease monotonically.

Thus here we consider adsorption processes involving competition between nucleation and growth of regular $c(2\times2)$ islands. At high Θ, in-phase islands coalesce on meeting to form ramified domains. We assume that a metastable saturation state results, with domains of different phase separated only by domain boundaries. Define the correlation length, ξ_0, as the separation at which the pair correlations are reduced by, say, $\frac{1}{2}$. Then the characteristic linear size (number of adspecies) for individual growing islands scale like ξ_0 ($s_0\equiv\xi_0^2$). We ask the following question: Does the saturation state approach percolation with increasing island-forming propensity, i.e., do the saturation values of $R_{\rm av}/\xi_0$ and $s_{\rm av}/s_0$ diverge as $\xi_0\to\infty$? The following argument suggests that this is the case. Suppose that $s_{\rm av}$ is analytically extended above saturation, Θ_s, to determine a ghost percolation threshold, $\Theta_{\rm GP}$, which we *assume* is below $\frac{1}{2}$. Then clearly one has $\Theta_{\rm GP}-\Theta_s<\frac{1}{2}-\Theta_s=O(\xi_0^{-1})\to 0$ as $\xi_0\to\infty$, which implies that the saturation state percolates in this limit.

Specifically, here we introduce an island-forming propensity into the five-site model by assuming that the rate, k_i, for irreversibly filling an empty site (with all NN's empty) depends on the number, i, of filled 2nd NN sites.[5] A multiplicative (Eden) rate choice $k_i\propto\alpha^i$ ($k_i/k_0=\alpha$, $i\geq 1$) produces individual $c(2\times2)$ islands with diamond shape (roughly circular Eden cluster structure); $\alpha\geq 1$ measures the clustering propensity. The characteristic or correlation length, ξ_0, scales like $\alpha^{1/2}$ ($\alpha^{1/3}$), and thus $\frac{1}{2}-\Theta_s$ scales like $\alpha^{-1/2}$ ($\alpha^{-1/3}$), as $\alpha\to\infty$ for multiplicative (Eden) rates. See Ref. 5 for a detailed discussion of these results, and for pictures of the saturation state.

Direct analysis of $s_{\rm av}(\Theta)$, etc., and $\Theta_{\rm GP}$, for large α, is not practical here because domains become so large. Instead we study the $c(2\times2)$ percolation transition for 2NN domains obtained by biasing the rates $k_0^{\pm}=(1\pm\delta)k_0$ for nucleation of $\pm$ phase islands, but not the other growth and coalescence rates where $k_i^{\pm}=k_i$, for $i\geq 1$. Table II and Fig. 9 gives FSS results for the α dependence of the saturation-state critical bias, δ_c, indicating that $\delta_c\to 0$, as $\alpha\to\infty$, for both rate choices. Note the difficulty in achieving convergence, and need to use large lattices, for systems with larger ξ_0 (e.g., for $k_i\propto 16^i$, we ran 80, 400 and 2000 trials on 256×256, 128×128, and 64×64 lattices, respectively, and several thousand trials on smaller lattices). These results are compatible with the above picture of how the saturation state approaches percolation, since this implies that $\delta_c=O(\Theta_{\rm GP}-\Theta_s)=O(\xi_0^{-1})$, as $\xi_0\to\infty$. [This assumes that the percolation line has slope $O(1)$.] Since random percolation critical exponents are always found, this fur-

TABLE II. Determination of saturation critical bias for $c(2\times2)$ 2NN percolation in the five-site model with multiplicative (M) and Eden (E) rate choices; δ values satisfying $R_L(\delta)=2^{273/72}$ are shown.

α	$L=16$	$L=32$	$L=64$	$L=128$
1 (E,M)	0.207	0.216	0.215	
2 (E)	0.172	0.179	0.176	
5 (E)	0.151	0.137	0.126	
15 (E)		0.081	0.086	
100 (E)	0.050	0.036	0.046	
2 (M)	0.163	0.154	0.155	
5 (M)		0.086	0.088	0.091
16 (M)		0.042	0.027	0.048
64 (M)			0.02	0.01

ther implies that as $\alpha\to\infty$ and the saturation state domains approach percolation, the effective dimension of large domains approaches the random percolation threshold value of $\frac{91}{48}$.

One could construct complete percolation phase diagrams for these processes analogous to Sec. II. Here we just make a few observations. Clearly $\frac{1}{2}-\Theta_s(\delta\neq0)\leq\frac{1}{2}-\Theta_s(\delta=0)=O(\xi_0^{-1})\to0$, as $\alpha\to\infty$. The left end of the (ghost) percolation line $(\delta,\Theta)=(0,\Theta_{GP})$ is "sandwiched" between $(0,\Theta_s)$ and $(0,\frac{1}{2})$. The right end is given by $(\delta,\Theta)=(1,\Theta'(\alpha)/2)$, where $\Theta'(\alpha)$ denotes the percolation threshold for a process where *all* sites on a square lattice fill irreversibly with rates $k_i=k_i(\alpha)$ depending on the number, i, of filled NN sites. The $\Theta'(\alpha)$ have been determined previously.[15,16]

Finally we provide some direct analysis of $\alpha\to\infty$ domain structure recognizing that, in this limit, lattice $c(2\times2)$ island-growth processes become continuum two-phase grain-growth-type processes.[5,28,29] Here grains, representing individual islands, nucleate at constant rate at randomly chosen unconverted points in the plane; they are assigned one of two phases, $\pm$, with probabilities $p^{\pm}=(1\pm\delta)/2$; details of grain shape and growth depend on the specific (biased) $c(2\times2)$ island-forming model being considered. In any case, at completion of the process, i.e., at saturation, the plane is divided between territories of $+$ and $-$ phase. For such continuum systems, exactly one phase must percolate, unless both are at a common percolation threshold (cf. Ref. 30). Thus, by symmetry, for $\delta\gtrless0$, the $\pm$ phase percolates, and at $\delta=0$ both are at the percolation threshold. This conclusion is, of course, consistent with the above remarks.

It is instructive to consider, specifically, the (biased) Eden rate choice in the $\alpha\to\infty$ limit which becomes a biased two-phase Johnson-Mehl-type model:[5,28,29] grain nucleation and phase assignment is as described above; grains have essentially circular shape and expand at constant rate until impingement; thereafter free boundaries continue to expand at constant rate. Figure 10 shows this evolution and the resulting Johnson-Mehl tessellation of the plane for a random phase assignment ($\delta=0$). One can see how adjacent grains of the same phase connect to form ramified regions at saturation. We pursue these ideas further by constructing a random lattice dual to this Johnson-Mehl tessellation of the plane: grains are identified as sites; sites corresponding to neighboring grains are linked by bonds. We observe that, for $\delta=0$, like-phase domains are at the percolation threshold if and only if the site percolation threshold, p_{sr}, of this random lattice equals $\frac{1}{2}$, the minimum allowed value.[31] Note that removing two-sided "lenses" from this tesselation does not effect the connectivity of this random lattice and produces an average coordination number of 6 (Euler's relation).[28] Thus we expect p_{sr} to equal $\frac{1}{2}$ by comparison with results for the random lattice dual to a Voronoi tessellation,[32] and for a triangular lattice.[22] Of course, this result also follows from the general arguments above, which furthermore imply that $p_{sr}=\frac{1}{2}$ for a broad class of random lattices generated by various grain-growth models. Standard random percolation critical exponents are also expected (cf. Ref. 32).

In closing this section, we briefly consider the growth of $c(2\times2)$ islands about randomly distributed seeds. Consider the continuum regime of low seed density. For circular islands, the saturation state is determined by appropriately assigning phases, $\pm$, to regions of the Voronoi tessellation associated with the seed distribution. For a random phase assignment, the analysis of the corresponding random lattice site percolation problem in Ref. 32 can be applied to show that this saturation state is at the percolation threshold. This result also follows from the general continuum percolation arguments described above.

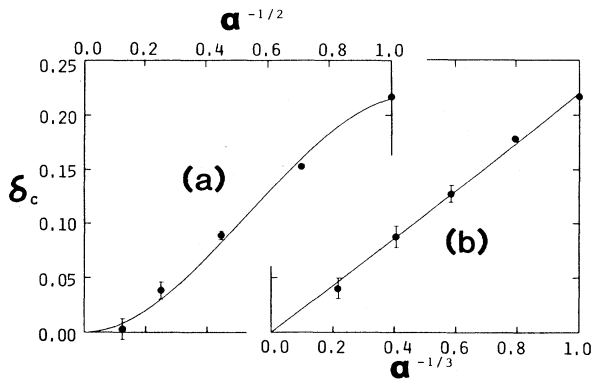

FIG. 9. Dependence of the saturation state critical bias δ_c on the clustering propensity α for the five-site model with a (a) multiplicative, (b) Eden rate choice.

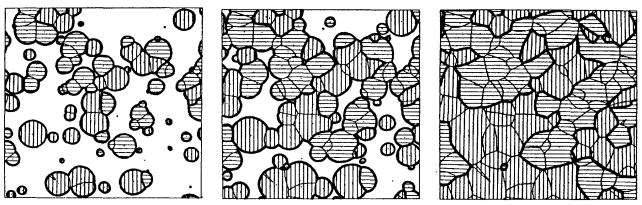

FIG. 10. Evolution the (unbiased) two-state Johnson-Mehl grain growth model. The horizontal or vertical cross hatching of grains represent the different phase choices.

V. SUMMARY AND EXTENSIONS

In this communication, we have considered simple models describing the development of $c(2\times2)$ short-range order during chemisorption. In previous work on these models, we have investigated the structure of the pair correlations and individual growing islands, and the diffracted intensity behavior. Here we have provided a quantitative analysis of the large-scale percolative adlayer structure, adapting ideas from correlated percolation theory. In particular, we have elucidated the coverage dependence of various measures of domain size through introduction of the new concept of "ghost percolation thresholds," occurring above saturation. This concept is elaborated further by obtaining, via FSS analyses, accurate percolation phase diagrams for classes of biased adsorption models incorporating the original model. Introducing a $c(2\times2)$ island-forming propensity α shifts the saturation state closer to percolation. This behavior is elucidated by analyzing two-phase grain growth models for the $\alpha\rightarrow\infty$ limit using ideas of stochastic geometry and continuum and random lattice percolation theory. The basic structure in these models is always dictated by the random percolation universality class. Consequently, we also expect to see this type of structure for a much broader class of models describing disordered $c(2\times2)$ adlayers.

In future work,[33] we shall analyze the large-scale fractal structure of the saturation state domain boundaries. We shall determine whether these can be described by suitably correlated self-avoiding-type walks (cf. Ref. 34), with correlations reflecting local adlayer statistics. In a separate communication,[35] we shall analyze the percolative characteristics of the disordered $c(2\times2)$ equilibrium distributions associated with the hard-square lattice gas. It has been asserted that a percolation transition in the Ising model universality class occurs here at the critical coverage for AB connectivity.[7] This change in universality class might be anticipated since the correlation length diverges at the critical coverage. In contrast, the pair correlations in filling models always have finite range with superexponential asymptotic decay.[36] Another focus of this work will be to exploit further ideas of analytic extension used above in connection with ghost percolation. Specifically, such ideas shall be used to elucidate the behavior of chord length measures of domain size in these $c(2\times2)$ filling models.[35]

Note that island coalescence, which is responsible for the percolative structure described above, is greatly reduced with increasing degeneracy (number of phases) of the ordered regions. Consider the development of four-phase $p(2\times2)$ short-range order on a square lattice. For a model where sites fill randomly only when all NN's and second NN's are empty, simulations reveal saturation states with small, stringy $p(2\times2)$ domains, and Θ_s very close to the "generalized Palisti conjecture" estimate of $(1-e^{-2})^2/4\sim0.1869$.[6,26] For a process where circular $p(2\times2)$ islands nucleate continuously and expand at constant rate, the saturation state structure is determined by randomly assigning one of four phases to regions in a Johnson-Mehl tessellation. Linkage of adjacent like-phase regions is limited. In fact, phase assignments exist which produce no linkage (the *four-color problem*).[37]

ACKNOWLEDGMENTS

Ames Laboratory is operated for the U.S. Department of Energy by Iowa State University under Contract No.W-7405-Eng-82. Johnson-Mehl grain patterns were provided by H. J. Frost, C. V. Thompson, and C. L. Howe.

[1]L. D. Roelofs, in *Chemistry and Physics of Solid Surfaces*, edited by R. Vaneslow and R. Howe (Springer, Berlin, 1982), Vol. 4; T. L. Einstein, in *ibid.*

[2]J. D. Gunton and K. Kaski, Surf. Sci. **144**, 290 (1984).

[3]M. G. Lagally, G.-C. Wang, and T.-M. Lu, in CRC Crit. Rev. Solid State Mater. Sci. **7**, 233 (1978).

[4]E. D. Williams, W. H. Weinberg, and A. C. Sobrero, J. Chem. Phys. **76**, 1150 (1982); E. S. Hood, B. H. Toby, and W. H. Weinberg, Phys. Rev. Lett. **55**, 2437 (1985).

[5]J. W. Evans and R. S. Nord, J. Vac. Sci. Technol. A **5**, 1040 (1987); J. W. Evans, R. S. Nord, and J. A. Rabaey, Phys. Rev. B **37**, 8598 (1988).

[6]J. W. Evans, J. Chem. Phys. **87**, 3038 (1987).

[7]G. Monroy, F. diLiberto, and F. Peruggi, Z. Phys. B **49**, 239 (1982); F. Peruggi, F. diLiberto, and G. Monroy, Physica **123A**, 175 (1984).

[8]F. Peruggi, Physica **141**, 140 (1987).

[9]A. Coniglio, C. R. Nappa, F. Peruggi, and L. Russo, J. Phys. A **10**, 205 (1977).

[10]D. Stauffer, *Introduction to Percolation Theory* (Taylor and Francis, London, 1985).

[11]H. P. Peters, D. Stauffer, H. P. Hölters, and K. Loewenich, Z. Phys. B **34**, 399 (1979).

[12]D. Stauffer, A. Coniglio, and M. Adam, in *Advances in Polymer Science* (Springer, Berlin, 1982), Vol. 44.

[13]A. L. R. Bug, S. A. Safran, G. S. Grest, and I. Webman, Phys. Rev. Lett. **55**, 1896 (1985).

[14]J. Lebowitz and H. Saleur, Physica **138A**, 194 (1986).

[15]J. W. Evans and D. E. Sanders, J. Vac. Sci. Technol. A **6**, 726 (1988).

[16]D. E. Sanders and J. W. Evans, Phys. Rev. A **38**, 4186 (1988).

[17]H. Saleur and B. Derrida, J. Phys. **46**, 1043 (1985).

[18]D. J. Dwyer, G. W. Simmons, and R. P. Wei, Surf. Sci. **64**, 617 (1977).

[19]J. Kertesz, B. K. Chakrabarti, and J. A. M. S. Duarte, J. Phys. A **15**, L13 (1982); P. Meakin, J. L. Cardy, E. Loh, D. J. Scalapino, J. Chem. Phys. **86**, 2380 (1987).

[20]J. W. Evans, D. R. Burgess, and D. K. Hoffman, J. Chem. Phys. **79**, 5011 (1983).

[21]D. K. Hoffman, J. Chem. Phys. **65**, 95 (1976); J. W. Evans, Physica A **123**, 297 (1984).

[22]D. Stauffer, Phys. Rev. Lett. **41**, 1333 (1978).

[23]Here $R_L(\delta)=2^{273/72}$ when $\delta=0.064,0.064,0.065$, for $L=16,32,64$, respectively.

[24]S.-L. Chang and P. A. Thiel, Phys. Rev. Lett. **59**, 296 (1987); S.-L. Chang, D. E. Sanders, J. W. Evans, and P. A. Thiel, in

The Structure of Surfaces II, Vol. 11 of *Springer Series in Surface Science,* edited by J. F. Van der Veen and M. A. Van Hove (Springer, Berlin, 1988).

[25]Here $R_L(\delta)=2^{273/72}$ when $\delta=0.204,0.174,0.166$, for $L=16,32,64$, respectively.

[26]See, e.g., R. S. Nord and J. W. Evans, J. Chem. Phys. **82**, 2795 (1985).

[27]For random dimer filling of NN sites on a square lattice, $R_L(\Theta)=2^{273/72}$ for filled (empty) clusters when $\Theta=0.5572,0.5619,0.5634,0.5615$ (0.440,0.436,0.433,0.434) for $L=8,16,32,64$, respectively. A Bunde, H. Harder, and W. Dieterich, Solid State Ionics **18/19**, 156 (1986), previously estimated the empty site percolation threshold at $\Theta=0.448\pm0.01$.

[28]A. Getis and B. Boots, *Models of Spatial Processes* (Cambridge, University Press, Cambridge, 1978).

[29]S. Ohta, K. Ohta and K. Kawasaki, Physica **140A**, 478 (1987).

[30]R. Zallen and H. Scher, Phys. Rev. B **4**, 4471 (1971); J. Kertesz, J. Phys. (Paris) Lett. **42**, L393 (1981).

[31]H. J. Frost and J. W. Evans (unpublished).

[32]J. F. McCarthy, J. Phys. A: Math. Gen. **20**, 3465 (1987).

[33]J. W. Evans (unpublished).

[34]R. M. Ziff, P. T. Cummings, and G. T. Stell, J. Phys. A **17**, 3009 (1984).

[35]J. W. Evans (unpublished).

[36]J. W. Evans, D. R. Burgess, and D. K. Hoffman, J. Math. Phys. **25**, 3051 (1984).

[37]K. Appel and W. Haken, in *Mathematics Today,* edited by L. A. Steen (Springer, New York, 1978).